THE IMPORTANCE OF CREATING DYNAMICALLY-SCALED MODELS OF AQUATIC VEGETATION IN THE LABORATORY

MARYAM ABDOLAHPOUR
School of Civil, Environmental and Mining Engineering, University of Western Australia, 135 Stirling Highway, Perth, WA 6009, Australia
School of Natural Sciences, Edith Cowan University, 270 Joondalup Drive, Joondalup, WA 6027, Australia

MARCO GHISALBERTI
School of Civil, Environmental and Mining Engineering, University of Western Australia, 135 Stirling Highway, Perth, WA 6009, Australia

PAUL LAVERY
School of Natural Sciences, Edith Cowan University, 270 Joondalup Drive, Joondalup, WA 6027, Australia

KATHRYN MC MAHON
School of Natural Sciences, Edith Cowan University, 270 Joondalup Drive, Joondalup, WA 6027, Australia

Physical modelling of vegetated flows is an essential component of process-based investigations into vegetation ecohydraulics. The vast majority of research into vegetated flows has employed rigid model vegetation, so that the canopy's geometry (i.e. its height and frontal area) is invariant and easy to quantify. Here, we demonstrate that embedding realism (in the form of flexibility and buoyancy) in the model vegetation can have a profound impact on the hydrodynamics. Specifically, we compare rates of vertical mixing in two types of model canopy (with identical heights and frontal areas) subjected to oscillatory flow over a range of realistic wave heights and periods. The two types of canopy were: (1) a rigid canopy consisting of wooden dowels, and (2) an array of flexible, buoyant model plants designed to mimic a meadow of the seagrass *Posidonia australis*. Dynamic similarity between the model and real seagrass was achieved by matching the two dimensionless ratios of the dominant forces that govern plant motion (rigidity, buoyancy and drag). Results demonstrate a significant difference in flow structure between the two canopies and a significant reduction in the rate of vertical mixing in a flexible canopy, relative to the rigid analogue. Thus, while the use of dynamically-scaled vegetation models adds a layer of modelling complexity, it represents a step towards a more faithful recreation of flow and mixing in these systems.

1 INTRODUCTION

Physical modelling of vegetated flows is essential in studying important hydrodynamic processes in canopy flows. It is crucial to ensure that the dynamically-scaled model maintains the important biomechanical behavior of the real vegetation in order to accurately represent the natural system. The vast majority of previous studies have modelled vegetation by using rigid elements in which the geometry is invariant and easily quantified. Although rigid cylinders are ideal to represent the stems of seagrass canopies [*Lowe et al.*, 2005], they may not successfully recreate situations where flexibility, buoyancy and configuration of the flexible plants are important [*Koehl et al.*, 2008; *Mass et al.*, 2010]. In particular, flexibility enables the plants to adapt their shape and posture in response to the flow fields. This allows the canopy to exert a time-varying roughness that may result in a substantial reduction in drag [*Rominger and Nepf*, 2014]. The issue of time-varying drag, which will introduce further complexity into the wave-dominated vegetated flows, can have many critical and beneficial implications in environmental studies such as the impact of blade posture on light availability [*Zimmerman*, 2003], nutrient uptake [*Hurd*, 2000] and oxygen transfer [*Mass et al.*, 2010]. Thus, the importance of creating a flexible, buoyant seagrass model was investigated in the context of predicting rates of vertical mixing.

Vertical mixing is typically the main process controlling vertical exchange of material into and out of coastal canopies. It therefore controls the large-scale ecological impact of, for example, seagrass meadows. Rates of vertical mixing were compared in the laboratory with two model canopies (rigid and flexible) that were otherwise identical. The same canopy height (h_c) and canopy dimensionless frontal area (ad, where a is the

canopy frontal area per unit volume and d is the stem diameter) were examined for both cases so that the flexibility was the sole variable impacting the mixing rates.

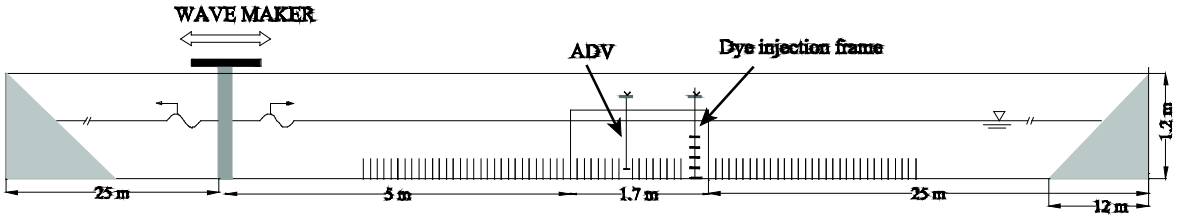

Figure 1. Schematic view of the experimental configuration in the wave tank. Not to scale.

2 METHODS

Experiments were conducted in a 50 m long, 120 cm wide, and 120 cm deep tank (Figure 1) with a piston-type wavemaker located in the middle of the tank. Beaches of slope 1:10 were constructed at both ends of the tank to minimise the wave reflection (estimated as < 6%).

Two canopy dimensionless frontal areas (ad = 0.063 and 0.131, typical of aquatic vegetation [*Gambi et al.*, 1990; *Luhar et al.*, 2010]), were examined for both rigid and flexible vegetation. The rigid model plants consisted of 6.4-mm diameter birch dowels with 30 cm height and the flexible model plants were designed by matching the two dimensionless rations of the dominant hydrodynamic forces between the model and real blade as detailed in section 2.1.

Each canopy was exposed to nineteen flow conditions by varying the wave period (T = 5-9 s) and height (H = 6-18 cm).

2.1 Design of flexible vegetation

The drag (F_D), buoyancy (F_B) and rigidity (F_R) forces of the seagrass define the plant motion. Therefore, dynamic similarity between the model and real vegetation can be achieved by matching the two dimensionless ratios of these forces [*Marco Ghisalberti and Nepf*, 2002]. The first is a ratio of buoyancy force to rigidity force (λ_1):

$$\lambda_1 = \frac{F_B}{F_R} = \frac{(\rho_w - \rho_s) g {h_c}^3}{Et^2} \quad (1)$$

where ρ_w, ρ_s and t are the density of water, the density of the seagrass and the blade thickness, respectively. E is the modulus of elasticity of the blade and measures the resistance of the blade to deformation. A stiffer blade will have a greater modulus of elasticity, a higher restoring force due to the rigidity and ultimately a lower λ_1. That is a blade at low λ_1 represents a cantilever-like motion and a blade at high λ_1 represents a buoyancy dominated motion. The second dimensionless ratio is the ratio of drag force to the rigidity force (λ_2):

$$\lambda_2 = \frac{F_D}{F_R} = \frac{\rho_w h_c U_c^2}{Et^3} \quad (2)$$

where U_c is the depth-averaged velocity within the canopy. Note that λ_2 is the Cauchy number ($Ca = C_d \rho_w h^3 U_c^2 / 2Et^3$, where C_d is the drag coefficient) and sets the posture of the blade such that the rate at which the blade will be bent over is dictated by the relative magnitude of drag and rigidity force [*Luhar and Nepf*, 2011]. In other words, a blade with greater λ_2 (or *Ca*) will be pushed over more easily than a blade with lower λ_2.

Therefore, dynamic similarity between the model and real plants requires that $\lambda_{1m} = \lambda_{1p}$ and $\lambda_{2m} = \lambda_{2p}$ (where the subscript *m* indicates the model and subscript *p* indicates the prototype). This has been achieved through mathematically and visually matching λ_1 and λ_2, respectively.

The average *Posidonia australis* values of $h_c \simeq$ 34 cm ($\simeq$ 27 – 43 cm), $t \simeq$ 0.29 mm ($\simeq$ 0.21 – 0.41 mm), $b \simeq$ 1 cm ($\simeq$ 0.92 – 1.1 cm, where b is the blade width) and W = 1 g ($\simeq$ 0.6 – 1.7 g, where W is the blade weight)

were estimated based on the measurements done on 50 seagrass blades collected from two different sites (Cockburn Sound & Shoalwater Bay) in Western Australia. Note that we assumed a constant blade width and thickness over its height so that $\rho_s \simeq 860$ kg/m^3 ($\simeq 750 - 970$ kg/m^3) was obtained for the *P. australis* leaves examined here. Since, there is no accurate estimation of *E* for *Posidonia australis* blades, the elastic modulus of *Zostera marina* (a structurally and morphologically similar species), *E* = 0.4 - 2.4 GPa [*Bradley and Houser*, 2009; *Luhar and Nepf*, 2011] was applied in our calculations. By assuming ρ_w = 1025 kg/m^3 for the density of seawater, λ_{1p} attained the average value of 0.12.

Trial plants with different heights and thicknesses were cut from Low Density Polyethylene (LDPE, ρ_s= 920 kg/m^{-3}) to cover a range of λ_{1m} values from 0.04 to 0.4. Each leaf was a 1-cm wide strip attached to a 3-cm wooden dowel at the base in order to simulate the stiffness of the stem. Artificial seagrass leaves along with a typical real *P. australis* leaf were subjected to different wave conditions in the flume to visually determine the most realistic model plant motion (Figure 1).

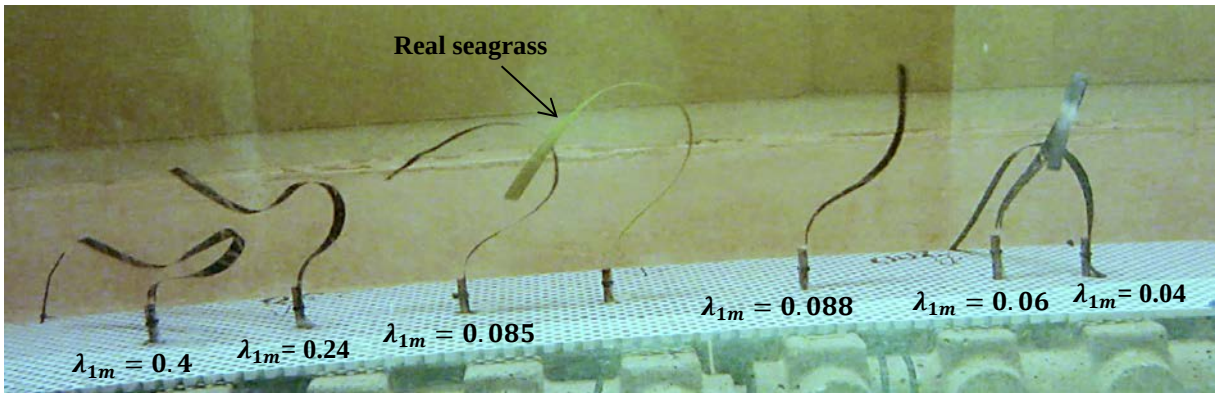

Figure1. The behavior of model seagrass leaves with $\lambda_{1,m} \simeq 0.4$ to 0.04 in comparison with the real *P. australis* leaf. The model blade with $\lambda_{1,m} = 0.085$ exhibits the most realistic motion.

As seen in Figure 1, the plant with $\lambda_{1,m}$ = 0.085 showed the most realistic behavior. This was not unexpected, given our estimate of $\lambda_{1p} \simeq 0.12$. Therefore, this plant (with $\lambda_{1,m}$ = 0.085, *h* = 30 cm and *t* = 300 μm) was chosen as the optimal design.

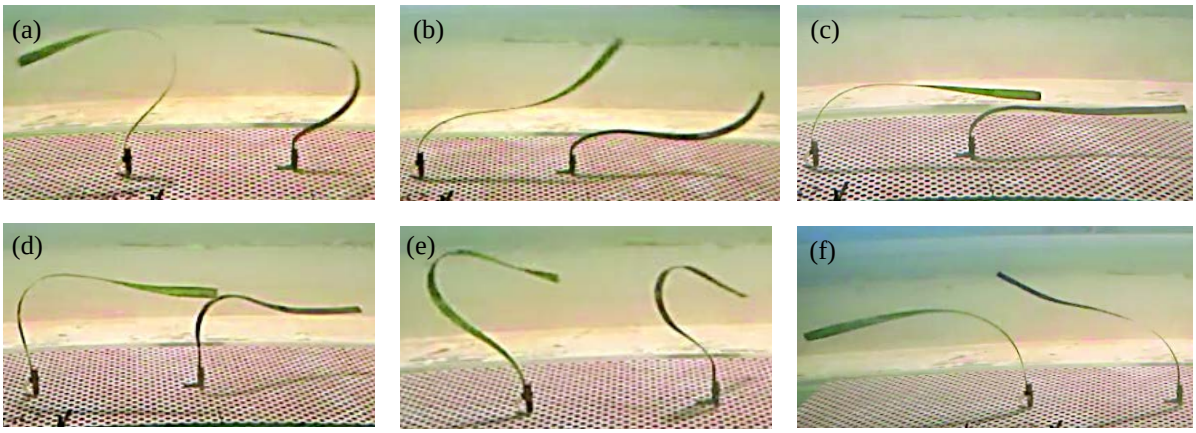

Figure 2. Comparison of the real and designed blades under different wave cycles. Figures 2a to 2c display the behaviour of the designed seagrass blade when the fluid motion is from left to right and Figures 2d to 2f display the blade motion when the fluid motion is from right to left. The real seagrass leaf is on the left hand side in all photos.

Importantly, the plant with $\lambda_{1,m}$ = 0.088 did not behave in a similar fashion as the real plant in all wave phases, despite having a comparable $\lambda_{1,m}$ as the selected plant (see Figure 1). This confirms the significant impact of λ_2 (or *Ca*) on plant motion as discussed earlier. Figure 2 illustrates the excellent similarities observed between the model and real blade under different phases of the surface waves.

2.2 Rigid and flexible canopy

6.4-mm diameter birch dowels (with 30 cm height) were inserted into perforated PVC boards and extended wall-to-wall, in order to construct the rigid canopy (Figure 3a). Each flexible plant was made of two blades with different heights (30 and 20 cm) attached to a stem like base in order to mimic the real *P. australis* shoot. The plants were then hammered into PVC boards and extended wall-to-wall as has been done for rigid vegetation (Figure 3b). The canopy length, L_c, varied from 3 to 6 m so that $L_c > 8\,A_\infty$ (where A_∞ is the horizontal particle excursion length). The dye injection setup was placed in the mid-length of the canopy as shown in Figure 3.

Figure 3. Photographs showing examples of (a) rigid and (b) flexible canopy as well as the dye injection setup was placed mid-length of the canopy in both cases.

2.3 Vertical mixing measurements

The vertical turbulent diffusivity ($D_{t,z}$) was measured through the evolution of vertical profiles of concentration (C) of a dye sheet injected into a wave-canopy flow. We define x as the direction of wave propagation, y as the lateral direction and z as the vertical direction (positive upward), with $z = 0$ at the bed (Figure 1). For a dye sheet mixed uniformly in the horizontal (i.e. $\partial C/\partial x = 0$ and $\partial C/\partial y = 0$) with no vertical advection, the solution to the mass transport equation for an instantaneous release at time $t = 0$ is given by a Gaussian distribution of concentration. The variance of the concentration distribution (σ^2) along any vertical line through the cloud will grow linearly with time, such that

$$\frac{d\sigma^2}{dt} = 2D_{t,z} \tag{3}$$

As a consequence, measurement of the rate of change of the variance of the vertical concentration distribution over time will allow the estimation of a vertical turbulent diffusivity [see e.g. *Fischer*, 1979 for more details]. A vertical array of 5 Turner Designs Cyclops 7 submersible fluorometers (every 15 cm, starting from the bed, Figure 3a) was used to measure the instantaneous concentration distribution (and variance) of the injected sheet of Rhodamine WT.

3 RESULTS

A comparison between the rates of vertical mixing in rigid and flexible vegetation demonstrates a lower $D_{t,z}$ in flexible vegetation (Figure 4). This strongly suggests that flexibility has a significant quantitative impact on flow and mixing in canopy flows.

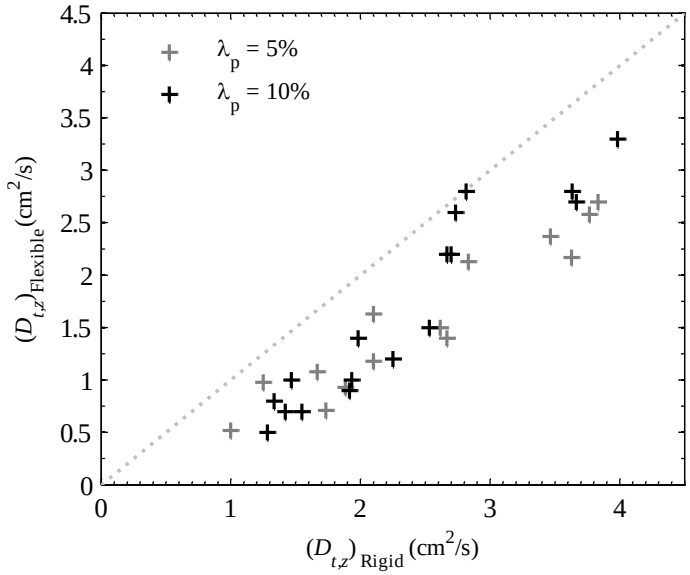

Figure 4. Values of vertical turbulent diffusivity, $D_{t,z}$, observed within a flexible canopy plotted against $D_{t,z}$ observed within a rigid canopy. $D_{t,z}$ values are almost always lower within a flexible vegetation.

Figure 5 illustrates how the canopy posture is altered by the magnitude of *Ca*. As can be seen, a lower *Ca* will lead to a greater change in canopy height (i.e lower h_d/h, where h_d is the minimum deflected height that canopy attains) which suggests the significant impact of F_D on plant posture (Eq. 2). Since F_R is constant throughout the experiments, the blades will achieve a lower h_d/h by increasing F_D (and consequently by increasing the *Ca*). It is therefore evident that *Ca* is a key parameter controlling the rate at which blades are bent over.

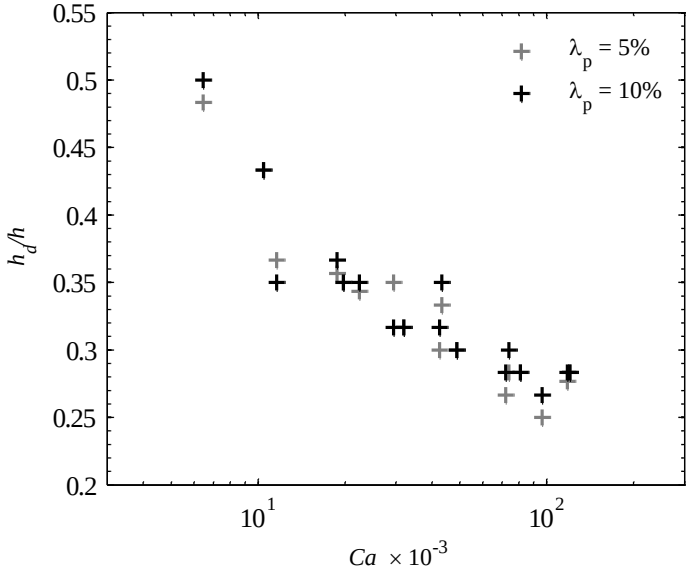

Figure 5. The relative magnitude of canopy deflected height and its actual height (h_d / h) plotted against Cauchy number (*Ca*). The canopy represents a greater deflection at higher *Ca* values.

Additionally, since increasing *Ca* leads to a greater canopy deflection we expect a greater variation in mixing values between rigid and flexible canopies when *Ca* is high. This, counterintuitively, is not supported by Figure 6 where the relative magnitude of vertical turbulent diffusivities in the flexible and rigid canopies, $(D_{t,z})_{\text{Flexible}}$ / $(D_{t,z})_{\text{Rigid}}$, tends to increase as *Ca* rises.

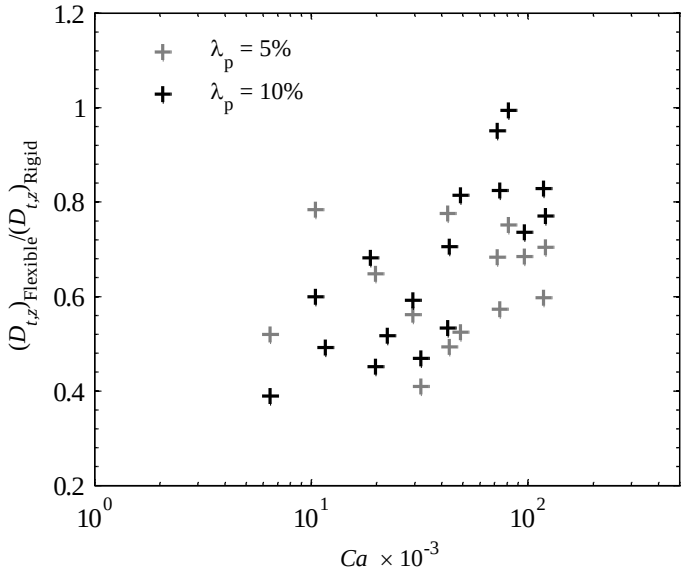

Figure 6. Flexible to rigid diffusivity values plotted against *Ca*. The $(D_{t,z})_{\text{Flexible}}$ / $(D_{t,z})_{\text{Rigid}}$ values, unexpectedly, increases by increasing *Ca*.

4 DISCUSSION

Our results revealed that the plant flexibility has a significant impact on mixing. The rates of vertical turbulent diffusivity within flexible vegetation were always lower than rigid vegetation in comparable wave and canopy conditions. In fact, flexible blades adjust their posture in response to the ambient flow, such that the relative velocity between the blade and flow reduces compared to the rigid, upright elements. This leads to the reduction of canopy drag, and subsequently the reduction of shear at the top of the canopy. This shear (from which vortex generation is expected [*Kundu and Cohen*, 1990]), is known to predominantly control the rate of vertical mixing in submerged canopies [*M Ghisalberti and Nepf*, 2002; *M Ghisalberti and Schlosser*, 2013; *Raupach et al.*, 1996]. Therefore, a weaker shear layer will result in a weaker vortex structure and finally a lower rate of vertical mixing (Figure 4).

Regardless of the considerable impact that flexibility can have on the hydrodynamics of the flow and the mixing rate, our results confirm the importance of creating dynamically scaled-models in vegetated flow studies. It is well understood that plants with different characteristics (in particular with different λ_1 and λ_2), can have different responses to the hydrodynamic forces and therefore may represent different behaviors. Although flexible-buoyant vegetation introduces a layer of complexity to the system, it is thus crucial to ensure the physical models in the laboratory faithfully recreate the hydrodynamics observed in real conditions.

5 REFERENCES

[1] Lowe, R. J., J. R. Koseff, and S. G. Monismith, "*Oscillatory flow through submerged canopies: 1. Velocity structure*", Journal of Geophysical Research: Oceans (1978–2012), (2005).

[2] Koehl, M., W. Silk, H. Liang, and L. Mahadevan, "*How kelp produce blade shapes suited to different flow regimes: a new wrinkle*", Integrative and Comparative Biology, 48(6), (2008), 834-851.

[3] Mass, T., A. Genin, U. Shavit, M. Grinstein, and D. Tchernov, "*Flow enhances photosynthesis in marine benthic autotrophs by increasing the efflux of oxygen from the organism to the water*", Proceedings of the National Academy of Sciences, 107(6), (2010), 2527-2531.

[4] Rominger, J. T., and H. M. Nepf, "*Effects of blade flexural rigidity on drag force and mass transfer rates in model blades*", Limnol Oceanogr, 59(6), (2014), 2028-2041.

[5] Zimmerman, R. C., "*A biooptical model of irradiance distribution and photosynthesis in seagrass canopies*", Limnol Oceanogr, 48(1part2), (2003), 568-585.

[6] Hurd, C. L., "*Water motion, marine macroalgal physiology, and production*", Journal of Phycology, 36(3), (2000), 453-472.

[7] Gambi, M. C., A. R. Nowell, and P. Jumars, "*Flume observations on flow dynamics in Zostera marina(eelgrass) beds*", Marine ecology progress series. Oldendorf, 61(1), (1990), 159-169.

[8] Luhar, M., S. Coutu, E. Infantes, S. Fox, and H. Nepf, "*Wave-induced velocities inside a model seagrass bed*", Journal of Geophysical Research: Oceans (1978–2012), (2010), 115(C12).

[9] Ghisalberti, M., and H. M. Nepf, "*Mixing layers and coherent structures in vegetated aquatic flows*", Journal of Geophysical Research, 107(C2), (2002).

[10] Bradley, K., and C. Houser, "*Relative velocity of seagrass blades: Implications for wave attenuation in low-energy environments*", Journal of Geophysical Research: Earth Surface (2003–2012), 114(F1), (2009).

[11] Luhar, M., and H. M. Nepf, "*Flow-induced reconfiguration of buoyant and flexible aquatic vegetation*", Limnol Oceanogr, 56(6), (2011).

[12] Fischer, H. B., "*Mixing in inland and coastal waters*", Access Online via Elsevier (1979).

[13] Kundu, P., and L. Cohen, "Fluid Mechanics", 638 pp, Academic, Calif. (1990).

[14] Ghisalberti, M., and T. Schlosser, "*Vortex generation in oscillatory canopy flow*", Journal of Geophysical Research: Oceans (2013).

[15] Raupach, M., J. Finnigan, and Y. Brunei, "*Coherent eddies and turbulence in vegetation canopies: the mixing-layer analogy*", Bound-Lay Meteorol, 78(3-4), (1996), 351-382.